Inorg. Chem. **2005**, *44*, 8999–9006

Redox Properties of Wild-Type and Heme-Binding Loop Mutants of Bacterial Cytochromes *c* Measured by Direct Electrochemistry

Tao Ye,[†] Ravinder Kaur,[‡] Xin Wen,[‡] Kara L. Bren,[‡] and Sean J. Elliott*[,†]

Department of Chemistry, Boston University, Boston, Massachusetts 02215, and Department of Chemistry, University of Rochester, Rochester, New York 14627-0216.

Received June 20, 2005

We have used protein film voltammetry (PFV) to determine the midpoint potentials of the *Pseudomonas aeruginosa, Hydrogenobacter thermophilus,* and *Nitrosomonas europaea* wild-type monoheme cytochromes *c* (cyts *c*; PA, HT, and NE, respectively), as well as PA N64Q, HT Q64N, and NE V65Δ mutants, as a function of pH, and buffer conditions. Recent studies have suggested that the identity of the 64 position of the heme-binding loop (either Asn or Gln) strongly influences the conformation of the Met ligand that binds the heme iron. The PFV studies reveal that HT and NE possess significantly lower potentials (wild-type cyts *c* having E_m values of +227 and +250 mV vs SHE) than PA (+290 mV) in 50 mM phosphate buffer, pH 7 at 3 °C. The HT Q64N mutant rises in potential compared to wild-type, and the PA N64Q mutant has a lower potential, indicating relationships between Met ligand fluxion, hydrogen bonding to the Met ligand, and redox chemistry. Surprisingly, NE V65Δ, possessing a heme binding loop nearly identical to that of the PA protein, displayed an E_m of + 232 mV, even lower than wild-type NE. These data are discussed in terms of models of Met ligand properties and proton dependence.

Introduction

Cytochromes *c* (cyts *c*) are among the most studied electron transfer (ET) proteins in terms of protein folding, electronic structure, ET kinetics, and thermodynamics. The electronic properties of the cyt *c* His−Met coordination environment are modulated by a variety of mechanisms, and recently, conformational dynamics of the heme-binding methionine side-chain residue has been described for a series of bacterial mono-heme cyt *c* proteins. In ^{1}H NMR studies, a subclass of members of the cyt c_8 structural family was found to display a unique compression of the typical range of heme methyl chemical shifts. Specifically, the oxidized state of analogous *Hydrogenobacter thermophilus* and *Nitrosomonas europaea* cyts c_{552} (HT and NE, respectively) both display an unusual compression of shifts,[1,2] as compared to prototypical members of the same family, e.g., the *Pseudomonas aeruginosa* cyt c_{551} (PA). The unusual electronic structure and NMR properties of HT and NE have been ascribed to "fluxional" behavior of the iron-binding Met side-chain residue, wherein the HT and NE cyts *c* Met residues sample two distinct conformations on the microsecond time scale (A and B in Figure 1).[3,4] In contrast, the analogous Met residue possesses a single conformation in PA,[5] the conformation that is typical of members of the cytochrome c_8 family (Figure 1B).

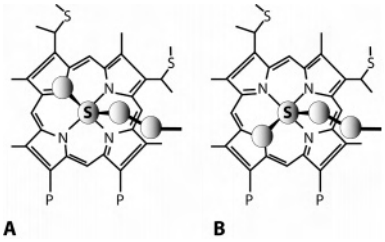

Figure 1. Typical conformation of an axial Met ligand at a heme *c* in (A) mitochondrial cyts *c*, (B) PA cyt c_{551}. The fluxional Met ligands observed in HT and NE allow rapid interconversion between the conformation depicted in (A) and (B). P indicates propionate.

Presently, there is no clear rationale for the differences in the Met ligand conformation and dynamics among cyts *c*.

* To whom correspondence should be addressed. E-mail: elliott@bu.edu.
[†] Boston University.
[‡] University of Rochester.

(1) Timkovich, R.; Cai, M. L.; Zhang, B. L.; Arciero, D. M.; Hooper, A. B. *Eur. J. Biochem.* **1994**, *226*, 159−168.
(2) Karan, E. F.; Russell, B. S.; Bren, K. L. *J. Biol. Inorg. Chem.* **2002**, *7*, 260−272.
(3) Zhong, L.; Wen, X.; Rabinowitz, T. M.; Russell, B. S.; Karan, E. F.; Bren, K. L. *PNAS* **2004**, *101*, 8637−8642.
(4) Bren, K. L.; Kellogg, J. A.; Kaur, R.; Xin, W. *Inorg. Chem.* **2004**, *43*, 7934−7944.
(5) Matsuura, Y.; Takano, T.; Dickerson, R. E. *J. Mol. Biol.* **1982**, *156*, 389−409.

10.1021/ic051003l CCC: $30.25
Published on Web 11/03/2005

In the case of PA and HT, mutational studies have indicated an important role for residue 64 (PA numbering) in the axial Met-donating loop. Residue 64 in most cyts c_8 is a conserved Asn that packs against the axial Met61 side chain and is positioned to donate a hydrogen bond to the Met sulfur. In HT, however, residue 64 is Gln, and analysis of the HT structure reveals that Gln64 is not positioned to hydrogen bond with Met61, but rather is pointed toward the protein surface.[3,6,7] Substitution of Gln for Asn64 in HT was shown to fix Met61 into a single conformation (Figure 1B), giving a PA-like electronic structure and heme pocket structure.[8] The complementary N64Q mutation in PA has subsequently been shown to induce axial Met fluxion, giving an NMR spectrum similar to that of HT.[8] The residue at position 64, however, is not the only factor determining Met conformation. In the Met-bearing loop of NE, residue 64 is an Asn that is positioned to interact with the axial Met, but the loop also contains an insertion at position 65 (Val 65), and the structure reveals that the NE Met-donating loop may pack against the heme in a distinct fashion, as compared to the HT and PA proteins. The fluxionality of the NE Met may also be tied to redox chemistry: while the studies of Bren and co-workers on the oxidized protein indicate fluxionality,[4] Timkovich and co-workers found a single conformation for the reduced form of the NE protein by ^{1}H NMR.[9] While the differences in Met ligand behavior have been clearly articulated through NMR studies, the impact of such behavior upon the functional chemistry of cyts *c* has not been determined.

Here, we address this by a systematic study of the reduction potential and electrochemical properties of wild-type HT and NE and compare them to PA, using the technique of protein film voltammetry (PFV). Additionally, we examine a series of three mutant cyts *c* that target the distinguishing features of the Met-donating loop in these proteins. To investigate the significance of variations in the Met-donating loop on functional properties of these cyts *c*, we have investigated PA N64Q, HT Q64N, and the NE V65 deletion mutant (V65Δ), which also possesses an Asn64 but removes the single insertion that makes the NE Met-bearing loop distinct from that in PA and HT.

To compare the redox chemistry of the six cyt *c* variants considered here, we have used PFV as a direct electrochemical tool to assess the midpoint potential (E_m) for the proteins. PFV allows for the direct and detailed analysis of thermodynamic and kinetic parameters of interfacial ET. In this experiment, protein molecules are adsorbed upon an appropriate electrode surface in a conformation that allows for fast ET of up to a monolayer of coverage. Noncovalent interactions are exploited in this method, such that the protein can maintain native structure and redox properties. In the case of cyt *c*, many recent studies have demonstrated that wild-type and mutant versions of yeast *iso*-1-cytochrome *c*[10] and cyt *c* from mammalian sources[11,12] are amenable to direct electrochemical studies using gold-based electrodes modified with either single- or mixed-component, self-assembled monolayers (SAMs) of alkane thiols.[13,14] As has been demonstrated in prior electrochemical studies, values of E_m and interfacial ET rate constants can be highly sensitive to the experimental parameters, including the terminal functionalities of the SAM, the chain length of the alkane thiol, and the ionic strength.[10,11,15] In particular, differences in observed E_m for bacterial cyts *c* have been ascribed to differences in experimental conditions.[16] Here, we have opted to use PFV to electrochemically interrogate the PA, HT, and NE wild-type and mutant proteins using a single electrode type, but under variable pH and ionic strength, to both discern the impact of the 64 position upon the potential, but also to uniformly explore the importance of pH and buffer conditions upon the observed electrochemistry.

Materials and Methods

Site-Directed Mutagenesis, Protein Expression, and Purification. Molecular biology procedures were carried out generally as described.[17] The expression and purification of the recombinant wild-type cyts *c*,[3,4,18] the HT Q64N,[19] and PA N64Q [8] were achieved as described previously. NE V65Δ was prepared as follows. The pSNEC expression plasmid (eq 4), was used as a template for site-directed mutagenesis using the PCR overlap extension method.[20] The mutagenic primers were 5′-GCCGCCAAACAACGTGAGC-GATG-3′ and 5′-CGCTCACGTTGTTTGGCGGCATT-3′. The fresh PCR product was cloned into the pCR2.1 vector (Invitrogen). Restriction digestion with *Bam*HI and *Nde*I (Promega or Gibco BRL) was performed to remove the gene insert from the pCR2.1 vector, which was subsequently cloned into the pSNEC vector to yield pSNECV65Δ (Amp^r) The gene sequence was confirmed by DNA sequencing. *Escherichia coli* strain BL21(DE3)-Star (Novagen) was transformed to ampicillin and chloramphenicol resistance with pSNECV65Δ and pEC86 (Cm^r), containing cyt *c* maturation genes,[21] and then used to inoculate 200 mL of LB medium in a 500-mL flask, supplemented with 50 μg/mL ampicillin and chloramphenicol. The culture was shaken for 10 h at 160 rpm, 37°C, and then used to inoculate 1 L of LB medium in a 4-L flask, which

(6) Hasegawa, J.; Yoshida, T.; Yamazaki, T.; Sambongi, Y.; Yu, Y.; Igarashi, Y.; Kodama, T.; Yamazaki, K.; Kyogoku, Y.; Kobayashi, Y. *Biochemistry* **1998**, *37*, 9641−9649.
(7) Travaglini-Allocatelli, C.; Gianni, S.; Dubey, V. K.; Borgia, A.; Di Matteo, A.; Bonivento, D.; Cutruzzolà, F.; Bren, K. L.; Brunori, M. *J. Biol. Chem.* **2005**, *280*, 25729−25734.
(8) Wen, X.; Bren, K. L. *Inorg. Chem.* **2005**, *44*, in press.
(9) Timkovich, R.; Bergmann, D.; Arciero, D. M.; Hooper, A. B. *Biophys. J.* **1998**, *75*, 1964−1972.
(10) El Kasmi, A.; Wallace, J. M.; Bowden, E. F.; Binet, S. M.; Linderman, R. J. *J. Am. Chem. Soc.* **1998**, *120*, 225−226.
(11) Song, S.; Clark, R. A.; Bowden, E. F.; Tarlov, M. J. *J. Phys. Chem.* **1993**, *97*, 6564−6572.
(12) Niki, K.; Hardy, W. R.; Hill, M. G.; Li, H.; Sprinkle, J. R.; Margoliash, E.; Fujita, K.; Tanimura, R.; Nakamura, N.; Ohno, H.; Richards, J. H.; Gray, H. B. *J. Phys. Chem. B* **2003**, *107*, 9947−9949.
(13) Arnold, S.; Feng, Z. Q.; Kakiuchi, T.; Knoll, W.; Niki, K. *J. Electroanal. Chem.* **1997**, *438*, 91−97.
(14) Sato, Y.; Mizutani, F. *J. Electroanal. Chem.* **1997**, *438*, 99−104.
(15) Wei, J. J.; Liu, H. Y.; Niki, K.; Margoliash, E.; Waldeck, D. H. *J. Phys. Chem. B* **2004**, *108*, 16912−16917.
(16) Terui, N.; Tachiiri, N.; Matsuo, H.; Hasegawa, J.; Uchiyama, S.; Kobayashi, Y.; Igarashi, Y.; Sambongi, Y.; Yamamoto, Y. *J. Am. Chem. Soc.* **2003**, *125*, 13650−13651.
(17) Sambrook, J.; Fritsch, E. F.; Maniatis, T. *Molecular Cloning: A Laboratory Manual*, 2nd ed.; Cold Spring Harbor Laboratory Press: New York, 1989.
(18) Russell, B. S.; Zhong, L.; Bigotti, M. G.; Cutruzzola, F.; Bren, K. L. *J. Biol. Inorg. Chem.* **2003**, *8*, 156−166.
(19) Wen, X.; Bren, K. L. *Biochemistry* **2005**, *44*, 5225−5233.
(20) Ho, S. N.; Hunt, H. D.; Horton, R. M.; Pullen, J. K.; Pease, L. R. *Gene* **1989**, *77*, 51−59.

was supplemented with antibiotics and shaken at 110 rpm, 37 °C for 18 h. Cells were harvested by centrifugation (5000*g*, 15 min, 4 °C), yielding a dark pink cell pellet. The cell lysis and protein purification were performed as described in ref 4.

NMR Spectroscopy. ^{1}H NMR spectra of NE V65Δ were collected on a Varian Inova 500-MHz spectrometer at 289 K. Oxidized protein (0.9 mM) was in 50 mM sodium phosphate, pH 6.0, 10% D_2O, with a 5-fold molar excess of $K_3[Fe(CN)_6]$. Recycle time was 250 ms.

Protein Electrochemistry. All PFV experiments were carried out using a PGSTAT 12 (Ecochemie) electrochemical analyzer, equipped with FRA and ECD modules. A three-electrode configuration was used in a water-jacketed glass cell. Temperature control was maintained using a refrigerating circulator. A platinum wire and resin-body calomel electrode (Accumet) were used as the counter and reference electrodes, respectively. Polycrystalline gold wire (2.0 mm diameter) embedded in epoxy comprised the working electrode. The gold electrode was polished mechanically with varying grits of alumina (1.0, 0.3, and 0.05 μm) to a mirror finish and then cleaned electrochemically in 0.1 M aqueous H_2SO_4 by cycling oxidatively over a range of potentials (0.2−1.35 V vs calomel). Electrochemically cleaned gold electrodes were then modified with a SAM of 6-mercaptohexanol by soaking the cleaned electrode in 1−2 mM ethanolic solution of the alkane thiol for 16 h. The excess alkane thiol was removed by rinsing with ethanol, followed by water, and was then considered ready for use. Protein films were achieved by directly adsorbing the cytochrome of interest (∼200 μM in pH 7.0 phosphate buffer) upon the electrode surface. Excess protein was removed with rinsing, and then the electrode was immersed in the prechilled electrochemical cell. Fast-scan rate experiments, which were required to determine interfacial ET rates, were carried out in a water-jacketed, all-glass electrochemical cell designed to allow for control of the location of the luggin-capillary with respect to the counter and working electrodes. Compensation for IR drop within the cell was further achieved by using by the IR positive feedback module of the PGSTAT 12 instrument. Cyclic voltammetry data were subjected to analysis by subtracting a polynomial baseline to remove the nonfarradaic current. The determination of interfacial ET constants was achieved by trumpet plot analysis (peak position of the cathodic and anodic electrochemical signals, as a function of scan rate), using the program Jellyfit, courtesy of Dr. Lars J. C. Jeuken.

Theory. The dependence of E_m upon phosphate ion concentration was investigated by applying the extended Debye−Hückel expression of the Nernst equation:

$$E_m = E_{m,I=0} + 2.303\frac{RT}{nF}[Z_{red}^2 - Z_{ox}^2]\frac{0.5\sqrt{I}}{1 + 3.3A\sqrt{I}} \qquad (1)$$

as has been described previously,[22−25] and used by Sola and coworkers.[26,27] In such a treatment, I is the ionic strength, $E_{m,I=0}$ is the redox potential at zero ionic strength (found by extrapolation),

(21) Arslan, E.; Schulz, H.; Zufferey, R.; Kunzler, P.; Thony-Meyer, L. *Biochem. Biophys. Res. Commun.* **1998**, *251*, 744−747.
(22) Tanford, C. *J. Am. Chem. Soc.* **1957**, *79*, 5340−5347.
(23) Margalit, R.; Schejter, A. *Eur. J. Biochem.* **1973**, *32*, 492−499.
(24) Gopal, D.; Wilson, G. S.; Earl, R. A.; Cusanovich, M. A. *J. Biol. Chem.* **1988**, *263*, 11652−11656.
(25) Moore, G. R.; Pettigrew, G. W. *Cytochromes c: Evolutionary, Structural and Physicochemical Aspects*; Springer-Verlag: New York, 1990.
(26) Battistuzzi, G.; Borsari, M.; Dallari, D.; Lancellotti, I.; Sola, M. *Eur. J. Biochem.* **1996**, *241*, 208−214.
(27) Battistuzzi, G.; Borsari, M.; Sola, M. *Arch. Biochem. Biophys.* **1997**, *339*, 283−290.

PA	59	IPMPP**N**-AVS	67
HT	57	VPMPP**Q**-NVT	65
NE	59	IPMPP**NV**NVS	68

Figure 2. Sequence alignment of a portion of the loop 3 region of PA, HT, and NE. The notable features of Asn or Gln in the 64 position (PA numbering scheme) and the insertion of Val 65 in the NE are highlighted as text in bold.

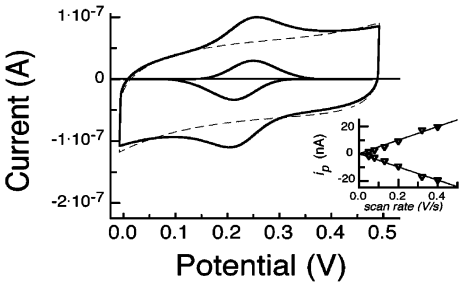

Figure 3. PFV response of HT wild-type upon mercaptohexanol-modified gold electrode. Raw data are shown (solid line, light) along with a baseline voltammogram of the electrode prior to cyt *c* adsorption (dash) and data baseline-subtracted to account for the nonfaradaic portion of the current (bold). Data were collected at pH = 6.5, 10 mM potassium phosphate buffer, 3 °C, υ = 50 mV/s. (Inset) The dependence of peak height (i_p) upon scan rate (υ), demonstrating a linear response, indicating that the PFV signal is due to an adsorbed species.

Z_{red} and Z_{ox} are the charges associated with the reduced and oxidized forms of cyt *c*, and *A* is the 'effective ionic diameter'.[23,24] By assuming an ionic strength function, $f(I)$, of

$$f(I) = (0.5\sqrt{I})/(1 + 3.3A\sqrt{I}) = (0.5\sqrt{I})(1 + 6\sqrt{I})$$

the relationship between potential, $f(I)$, and Z_{red} and Z_{ox} becomes

$$E_m = E_{m,I=0} + 2.303\frac{RT}{nF}[Z_{red}^2 - Z_{ox}^2]f(I) \qquad (2)$$

which predicts a linear relationship between $f(I)$ and E_m , with a slope of $(RT/nF)(Z_{red}^2 - Z_{ox}^2)$. Thus, ion binding to the either oxidation of the cytochrome results in a change in the net charge and in a detectable slope in a plot of $f(I)$ vs E_m is observed. Here, we use the observed slopes for the ionic strength dependence of E_m with respect to phosphate ion as a means to distinguish the NE and HT cyts *c*.

Results

Direct Electrochemistry. We have carried out the systematic direct electrochemical characterization of bacterial cyts *c*, PA, NE, and HT, as well as the heme-binding loop mutants PA N64Q, HT Q64N, and NE V65Δ. Successful cyclic voltammetry of (sub)monolayers was achieved upon gold electrodes modified with 6-mercaptohexan-1-ol. The bacterial cyts *c* studied here all give reproducible, stable electroactive protein films over a range of pH and ionic strength conditions. Representative data are shown for the HT wild-type protein in Figure 3, and baseline subtraction of the nonfaradaic portion of the current reveals a set of quasi-reversible peaks that display a small degree of peak separation. Protein films can be generated by direct deposition of a concentrated protein solution, with the removal of excess cytochrome, at 3 °C. All protein films give reversible signals of a highly symmetric shape. Plots of peak-height (i_p) vs. scan rate, shown in Figure 3 (inset), exhibit an excellent linearity, indicating that the protein is adsorbed.

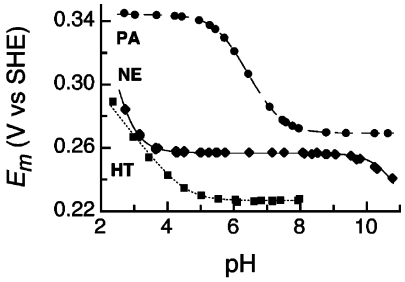

Figure 4. Influence of pH upon the midpoint potential E_m for PA (■), NE (◆), and HT (■), raw data were collected as described above.

In all cases reported here, the ratio of cathodic to anodic currents (i_c/i_a) was found to be approximately unity. Multiple scans of a given protein film indicate that film loss is minimal during the course of several experiments.

As described below, the reduction potential observed for each cytochrome was dependent upon the pH of the cell solution. It was also found that the use of phosphate buffer versus organic buffers (e.g., Tris, citrate, succinate, MOPS) gave rise to a systematic decrease in potential for the HT and NE proteins, which will be discussed further below.

To ensure that ET kinetics do not limit the observed electrochemical data, we determined the interfacial ET rate (k_0) using the methods of Laviron.[28] As described by Niki and co-workers,[29] the rates observed were somewhat dependent upon ionic strength. Rates of 175 s^{-1} were typical for the pH-dependence data given below.

pH Dependence. The influence of pH upon the midpoint potentials of wild-type cyts *c* is shown in Figure 4. As shown, PFV can be used to address a wide range of pH and to allow for the direct comparison of the pH-dependent redox properties of all of the cytochromes studied. We note that on the time scale of our experiments, shifts in E_m cannot be ascribed to protein unfolding in acidic or basic conditions, nor can the pH-dependent behavior represent the "alkaline form" of cyt *c*, which should have a much lower potential.[30] Protein films give reversible and reproducible results that do not depend on the order in which the various pH values are visited in the course of a single experiment.

As an important control, PA shows analogous behavior to that observed by Leitch and co-workers, using a spectrophotometric redox titration.[31] Our data (Figure 4, circles) are easily fit (dashed line) to the previously derived equation for two-state protonation chemistry (eq 3). Through the fitting, we have found pK_{red} and pK_{ox} values of 7.1 and 5.7, respectively.

$$E_m = E + 2.303\frac{RT}{nF}\log\left\{\frac{[H^+] + K_{red}}{K_{ox} + [H^+]}\right\} \qquad (3)$$

Our data are in good agreement with the findings of Leitch and co-workers (pK_{red} = 7.3 and pK_{ox} = 6.2),[31] and the discrepancies may be due to the tight coupling of proton and ET that can be better resolved in a PFV experiment.

NE displays a distinctive pH dependence that is present only at the extrema of pH (at pH values >9.25, <4.0). Largely invariant with pH, the NE data (Figure 4, diamonds) indicates that a singly protonated form of the cytochrome undergoes redox transformations and that this form can either deprotonate in the oxidized state or protonate further in the reduced state. Thus, the pH dependence at the extrema is approximately 54 mV/decade (at the temperatures studied in our experiments. The methods of Clark[32] can be used to determine that the appropriate pH dependence is described by eq 4

$$E_m = E + 2.303\frac{RT}{nF}\log\left\{\frac{[H^+]^2 + H^+K_{red} + K_{red}^2}{[H^+] + \dfrac{K_{ox}}{[H^+]}}\right\} \qquad (4)$$

Our data are similar in overall shape to that found by Barakat and Strekas for three cyts *c*′.[33] Here, we find ionizations occurring with p*K* values of pK_{red} = 2.8 and pK_{ox} = 10.7, unlike the closely spaced p*K* values for the cyts *c*′ (e.g., pK_{red} = 5 .4 and pK_{ox} = 8.0 for the *Rhodopseudomonas palustis* protein). The observed NE pH dependence is also similar to that found for bovine cyt *c* by Rodkey and Ball, though the mammalian protein demonstrates a steeper pH dependence at low pH values, indicating an additional protonation event of the reduced form (another pK_{red}).[34]

We found that HT wild-type appeared to be less suitable for an extensive pH dependence study, as compared to PA and NE. In our hands, HT protein films were found to be only stable using phosphate buffer, unlike the PA and NE proteins. Figure 4 shows that data (squares) could only be collected up to a pH of ~8.0. Aside from this hindrance, the overall appearance of the data is quite similar to the NE pH study, though the HT response is not identical. Fitting the response to eq 4 yielded satisfactory results (dotted line), though the assignment of pK_{ox} was not clear, as the protein films were not stable at sufficiently high pH to resolve a pK_{ox}. An alternative model, typical for the protonation chemistry of a reduced form of the cytochrome fits the data equally well, and is described by eq 5

$$E_m = E_{alk} + 2.303\frac{RT}{nF}\log\left\{1 + \frac{[H^+]}{K_{red}}\right\} \qquad (5)$$

In the case of either model, we found that the data was fit with pK_{red} = 4.5.

pH-Dependent Behavior of the Heme-Binding Loop Mutants. We have produced a detailed picture of the influence of the position 64 mutants upon cyt *c* redox chemistry as a function of pH. The results are summarized

(28) Laviron, E. *J. Electroanal. Chem.* **1979**, *101*, 19−28.
(29) Avila, A.; Gregory, B. W.; Niki, K.; Cotton, T. M. *J. Phys. Chem. B* **2000**, *104*, 2759−2766.
(30) Wilson, M. T.; Greenwood, C. In *Cytochrome c: a multidisciplinary approach*; Scott, R. A., Mauk, A. G., Eds.; University Science Books: Sausalito, CA, 1996; pp 611−634.
(31) Leitch, F. A.; Moore, G. R.; Pettigrew, G. W. *Biochemistry* **1984**, *23*, 1831−1838.
(32) Clark, W. M. *Oxidation−Reduction Potentials of Organic Systems*; The Williams and Wilkins Company: Baltimore, 1960.
(33) Barakat, R.; Strekas, T. C. *Biochim. Biophys. Acta* **1982**, *679*, 393−399.
(34) Rodkey, F. L.; Ball, E. G. *J. Biol. Chem.* **1950**, *182*, 17−28.

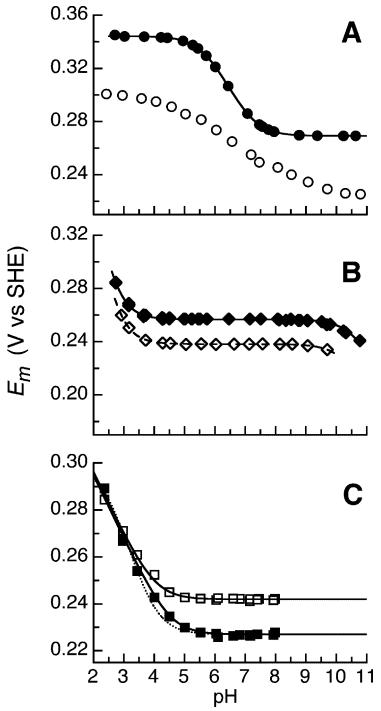

Figure 5. pH dependence of E_m for (A) PA (■) and PA N64Q (○); (B) NE (◆) and NE V65Δ (◇); (C) HT (■) and HT Q64N (□). Data were fit as described in the body of the text.

in Figure 5, which shows the dependencies for the three mutants, along with our attempts to fit the data with the following considerations.

PA N64Q. The PA mutant displays an overall shift downward in reduction potential upon mutation of Asn64 into Gln, rendering the mutant similar to the HT and NE proteins. Remarkably, the shift itself is pH dependent, and it is quite clear from Figure 5A that the sigmoidal fit displayed by PA wild-type, does not hold for PA N64Q. At pH extrema, the downward shift in potential is approximately −45 mV, yet at pH 7.5, the shift is just −22 mV. As described below, the transformation in the shape of the pH response can be interpreted in terms of a disruption of proton coupling or in a series of ionizations with p*K* values that sequentially shift the observed E_m throughout the near-neutral pH range.

HT Q64N. The HT mutant at the analogous 64 position displays an upward shift in midpoint potential of +15 mV between pH values of 5 and 8 (Figure 5C). The overall shape of the pH dependence is maintained, including one clearly resolved ionization associated with the reduced form of HT Q64N (pK_{red} = 4.0), as well as a very similar slope (∼25 mV/decade) at acidic pH values.

NE V65Δ. The NE deletion mutant removes a valine residue insertion (relative to the PA sequence) in the heme-binding loop, presumably making the ligand-bearing loop similar to the PA protein (Figure 2). Yet, as Figure 5B shows, the deletion of Val65 induced a *downward* shift in potential of approximately −20 mV, making the mutant appear to be quite similar in potential to the HT protein, yet the overall shape of the voltammogram is similar to the NE wild-type, including both pK_{red} and pK_{ox} values of 2.8 and 10.4, respectively (nearly identical to the p*K*'s of the wild-type, 2.8 and 10.7). As described below, ^{1}H NMR analysis of NE V65Δ suggest that the axial Met remains fluxional.

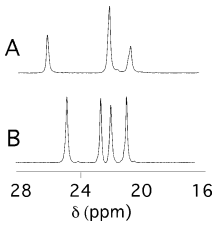

Figure 6. ^{1}H NMR spectra of oxidized NE V65Δ (A) and NE (B). The spectrum in (B) is from ref 4.

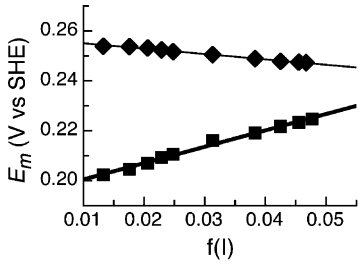

Figure 7. Midpoint potential dependence of phosphate ion concentration for NE (◆) and HT (■) wild-type proteins. Experiments were carried out at pH = 7.0, 0 °C, with a scan rate of 50 mV/s. Data are fit to eq 2, using a value of *A* of 1.8 nm.

NMR Study of the NE V65Δ Conformation. To investigate the impact of the NE V65Δ mutation upon the heme-binding loop structure, the NMR spectrum of the mutant was collected. Figure 6 shows the heme-methyl region of the ^{1}H NMR spectrum of the oxidized form of the mutant (A) and the wild-type (B) protein. The NE V65Δ spectrum clearly shows a compressed pattern of heme methyl resonances similar to NE and HT, an indicator of axial Met ligand fluxionality.[4] In a fashion similar to the redox properties described above, NE V65Δ appears to be unlike PA, which displays a large range of chemical shift values (∼20 ppm).[3]

Buffer Binding. As each of the three cyts *c* displayed a unique dependence upon pH, NE and HT also demonstrated sensitivity to the nature of the buffer in the cell solution. In particular, 50 mM phosphate buffer was found to induce a downward shift in potential of approximately −10 mV for both NE cyts *c*, as compared to organic buffers. For the NE proteins, the dependence of the midpoint potential in either phosphate or a set of organic buffers (citrate/succinate/Tris/MOPS/glycine) yield data that can be fit well by eq 3, and while pK_{red} is nearly identical, there is a notable shift in pK_{ox} (8.4 for phosphate buffer, versus 10.4 otherwise). For the HT proteins, the use of organic buffers appeared to give a poorly defined PFV response, as described above. In contrast with NE and HT, the PA and PA N64Q are not sensitive to the identity of the buffer.

To further compare NE and HT, the dependence of E_m upon phosphate ion concentration was investigated. Both cyts *c*, as well as their respective mutants, displayed an overall downward shift in potential at 50 mM phosphate, with respect to organic buffers (e.g., Tris, MOPS), yet Figure 7 shows the shift in E_m for NE and HT, as a function of the ionic strength, as the phosphate ion concentration from 1 to 50

mM. (Further changes in E_m were not observable at concentrations greater than 50 mM phosphate.) As shown in Figure 7, NE shows a negative slope while HT shows a positive slope, suggesting that the NE and HT cytochromes must differ in their charge and capacity for binding phosphate. An analysis of the ion binding for the HT cyt *c* indicates that $|Z_{red}| > |Z_{ox}|$. NE contrasts with this, the negative slope indicating that $|Z_{ox}| > |Z_{red}|$ and that the overall charge and/or phosphate-binding properties of the two cytochromes cannot be identical.

Discussion

We have demonstrated the impact of the composition of the axial Met-donating loop upon the redox chemistry of bacterial cyts *c*. By using PFV as an alternative to traditional bulk-phase voltammetry and/or potentiometic titration, we have been able to assess a series of cytochromes under highly controlled and homologous conditions. This systematic study allows us to pick apart the relative features of protein sequence and structure that control the reduction potential, as well as the protonation chemistry, of monoheme bacterial cyts *c*.

To date, this class of cytochromes has not been analyzed using PFV, though several direct voltammetric studies of immobilized eukaryotic analogues have been reported previously.[10−13,15,29,35−41] Our studies of midpoint potential of the wild-type cyts *c* (Figure 4) show that PFV gives a good agreement with previous reports achieved by either potentiometric redox titrations or bulk-phase electrochemistry. For example, the potential of PA has been reported by Moore and co-workers as +275 mV (at pH = 6.5)[42] and by Horio and co-workers as +289 mV.[43] We find that, at a similar pH, the value is +305 mV. The potential of the HT protein has been reported by Tomlinson and Ferguson as +245 mV by potentiometry[44] and as +224 mV by Ueyama and co-workers in a bulk-phase electrochemical study,[45] compared with our value at pH 7.0 of +227 mV. Further, HT demonstrates a similar decrease in potential due to phosphate ions, as has been reported for mitochondrial cyts *c*[24,26] and *R. palustris* cyt c_2,[27] as discussed by Sola and co-wokers.[46] PFV allows for the assessment of the same protein film under a wide range of conditions (pH, buffer composition, temperature) to determine the factors that contribute to the midpoint potential of cyts *c*. Notably, protein films appear as sub- or partial monolayers, where the observed values of E_m do not correlate with apparent electroactive coverage. Thus, upon the electrode surface, potential ionic interactions between neighboring cyt *c* molecules do not appear to contribute significantly to the observed values of E_m.

The 64 position in the bacterial cyt *c* heme binding loop is of particular interest due to the impact this residue may exert over Met ligand properties, including conformation and fluxionality and ability to act as a donor and/or acceptor. By studying the redox properties of a series of 64-position mutants, we have demonstrated that the Asn 64-containing proteins, such as the PA wild-type and HT Q64N, possess a higher midpoint potential than respective Gln 64-bearing analogues (PA N64Q and HT wild-type). This makes sense in terms of the proposed hydrogen-bonding interaction of N64 with the Met ligand. Structural characterization of PA reveals that N64 is positioned to hydrogen bond with M61 δS as well as the backbone carbonyl oxygen of I48 in the heme pocket,[5] whereas the Q64 residue of HT does not possess a conformation that allows for hydrogen bonding in either the oxidized or reduced state.[6] A correlation between hydrogen bonding to the Met ligand sulfur and the redox properties of the heme iron makes intuitive sense: when the Met ligand serves as a hydrogen-bond acceptor, Met should become a less-electron-rich ligand, which stabilizes the Fe(II) state of the heme, as compared to the Fe(III) state.[47] This effect should result in a *downward* shift in potential upon mutating Asn64 to Gln, removing the possibility of hydrogen bonding. Indeed, this was observed in the Y67F mutant of *Saccharomyces cerevisiae* iso-1-cyt *c*. Tyr67 donates a hydrogen bond to the axial Met80 δS in mitochondrial cyts *c*, and mutating this residue to Phe results in a variant with a redox potential 56 mV lower than that of wild-type.[47] In addition, a complementary case has been observed in imidazole complexes of metalloporphyrins: the free imidazole amine serves as a hydrogen-bond donor to an external molecule of base, which renders the ligand a *better* donor overall and results in a *downward* shift in redox potential of 40−60 mV.[48,49] Yet, the transformation of the Asn64 of the PA protein to Gln does not account for the entire difference between PA and HT. The mutation merely lowers the potential of PA N64Q by −30 mV (pH 7.0) with respect to wild-type, another −30 mV is required to match the Gln64-bearing HT protein. In addition, the change in potential is substantially less than is observed for *S. cerevisiae* Y67F iso-1-cyt *c* relative to wild-type. Similarly, the HT Q64N mutant does shift upward in potential by +15 mV, as compared to wild-type, which supports the importance of potential hydrogen-bonding interactions, yet this is still lower than the PA protein by ∼45 mV.

Alternatively, the NE proteins do not behave as might be expected from the simple model of hydrogen-bonding interactions to the axial Met. As Figure 2 depicts, the wild-

(35) Hinnen, C.; Niki, K. *J. Electroanal. Chem.* **1989**, *264*, 157−165.
(36) Sagara, T.; Niwa, K.; Sone, A.; Hinnen, C.; Niki, K. *Langmuir* **1990**, *6*, 254−262.
(37) Clark, R. A.; Bowden, E. F. *Langmuir* **1997**, *13*, 559−565.
(38) Imabayashi, S.; Mita, T.; Feng, Z. Q.; Iida, M.; Niki, K.; Kakiuchi, T. *Denki Kagaku* **1997**, *65*, 467−470.
(39) Leopold, M. C.; Bowden, E. F. *Langmuir* **2002**, *18*, 2239−2245.
(40) Nahir, T. M.; Bowden, E. F. *Langmuir* **2002**, *18*, 5283−5286.
(41) Tanimura, R.; Hill, M. G.; Margoliash, E.; Niki, K.; Ohno, H.; Gray, H. B. *Electrochem. Solid State Lett.* **2002**, *5*, E67−E70.
(42) Moore, G. R.; Pettigrew, G. W.; Pitt, R. C.; Williams, R. J. P. *Biochim. Biophys. Acta* **1980**, *590*, 261−271.
(43) Horio, T.; Higashi, T.; Sasagawa, M.; Kusai, K.; Nakai, M.; Okunuki, K. *Biochem. J.* **1960**, *77*, 194−201.
(44) Tomlinson, E. J.; Ferguson, S. J. *PNAS* **2000**, *97*, 5156−5160.
(45) Ueyama, S.; Isoda, S.; Hatanaka, H.; Shibano, Y. *J. Electroanal. Chem.* **1996**, *401*, 227−230.
(46) Battistuzzi, G.; Borsari, M.; Sola, M. *Eur. J. Biochem.* **2001**, 2989−3004.
(47) Berghuis, A. M.; Guillemette, J. G.; Smith, M.; Brayer, G. D. *J. Mol. Biol.* **1994**, *235*, 1326−1341.
(48) Quinn, R.; Mercer-Smith, J.; Burstyn, J. N.; Valentine, J. S. *J. Am. Chem. Soc.* **1984**, *106*, 4126−4144.
(49) O'Brien, P.; Sweigert, D. A. *Inorg. Chem.* **1985**, *24*, 1405−1409.

type NE protein sequence contains an Asn64 in homology to PA but also exhibits a unique insert of Val into the 65 position of the heme-binding loop. However, the Asn64 appears to be positioned correctly to engage in hydrogen bonding, as revealed by the NMR structure of the reduced protein.[9] Nevertheless, the NE protein is lower in potential than the PA wild-type at all pH values. Removal of the Val65 does not leave the NE V65Δ mutant more like the PA protein with respect to its redox potential. Instead, a downward shift of −19 mV is observed, and the NE V65Δ displays a nearly identical pH dependent behavior to the HT protein regardless of the difference in the identity of the residue at the 64 position. NE V65Δ also maintains a compressed heme methyl shift pattern in the oxidized form (Figure 6), suggesting that this inserted residue does not in itself explain the apparent Met fluxion in this protein. The observed downward shift in potential may be due to increased solvation of the heme moiety, as has been reported for cyt *c* models.[50]

The position-64 mutations in PA and HT affect the heme electronic structure significantly. HT wild-type and PA N64Q possess axial electronic structures, whereas PA wild-type and HT Q64N are rhombic.[3,8,19] In bis-His heme proteins and bis-imidazole porphyrins, it has been suggested that perpendicular alignment of the axial ligands may lead to a positive shift in redox potential of up to ∼50 mV over that observed for the parallel alignment.[51] In the cytochromes here in which the axial Met is sampling the two conformations shown in Figure 1, the average Met orientation would position the ligand, on average, perpendicular to the axial His. In the case of effectively parallel ligands relative to perpendicular ligands, the rhombic splitting parameter, *V*, is expected to be relatively small, while the tetragonal field parameter, Δ, does not change significantly. This results in a lower-energy, singly occupied molecular orbital and, thus, a higher redox potential. This effect may attenuate the decrease in potential for mutation of Asn64 to Gln in PA and also the increase in potential for mutation of Gln64 to Asn in HT, relative to what is expected on the basis of changes in hydrogen bonding to the axial Met. Note that the time scale of the Met fluxion (μs) is significantly shorter than the time scale of the PFV measurements.

The pH dependence of the cyts *c* reveal further subtleties. Using PFV, we observe a clear sigmoidal pH dependence for the PA WT. Notably, this response lacks the nonspecific pH-induced variations that are frequently observed at high and low pH values when using bulk-phase electrochemical methods.[52,53] We find pK_{ox} and pK_{red} values of 5.7 and 7.1 for the PA wild-type protein, typically associated with the redox influence of the protonation state of the heme propionate-7 (HP-7). However, we find that the N64Q mutant shows a dramatic disruption of proton coupling, yielding data that cannot be fit by the simple model associated with eq 3. Notably, recent studies from Yamamoto and co-workers have shown single and multiple PA mutations in proximity to HP-7 can greatly perturb the normal redox-linked p*K* values of the heme propionate side chains due to substantial lowering of pK_{red} and pK_{ox} values.[53] However, we find that the PA N64Q pH dependence cannot be accounted for in this way. The PA N64Q pH dependence instead suggests that either H^+/e^- has been greatly reduced, or a series of p*K* values are required to fit the data by typical procedures. The first of these possibilities appears more likely, although surprising, as it implies the N64 residue influences the ionization behavior of HP-7, greater than 10 Å away.

HT and NE do not reveal the sigmoidal pH dependence displayed by the PA proteins; instead, the cytochromes display an invariant midpoint potential at pH values close to neutral and one p*K* value at acidic pH values. HT and NE forms show similar pH dependencies, generally, with the exceptions that the HT proteins (wild-type and mutant) can only be studied by PFV over a limited range of basic pH values and NE proteins show a second p*K* at basic pH values. A further difference between the NE and HT forms is the extent of apparent stoichiometry of H^+/e^-. The NE proteins demonstrated a rigorous 1:1 H^+/e^- stoichiometry, as observed in the fitting of the data to a slope of 54 mV/decade in the linearly-dependent regions of the plot. However, the HT proteins demonstrated a slope of ∼27 mV/decade at low pH values, indicating that H^+/e^- coupling is reduced, assuming the model described by eq 5. A rationale for this difference is not readily apparent, though an alternative interpretation (Figure 5C, dotted line) attributes the pH dependence to a model like that of the PA proteins, described by eq 3.

Although similar, the redox properties of the NE and HT proteins are not identical, as demonstrated by the dependence of E_m upon phosphate concentration, which is suggestive of ion binding (Figure 7). Application of the traditional model using the Nernst equation and Debye−Hückel calculations [22−27] can quantify the difference in $|Z_{red}|$ and $|Z_{ox}|$, though the results of such analysis must be interpreted with care. Here, aspects of the simple Debye−Hückel model may not apply directly, particularly as the cytochrome molecules should be viewed as roughly spherical objects with charges uniformly distributed over their surface. However, bacterial cyts *c* do not display charge symmetrically, and it may be that the protein−electrode interaction further influences the display of charge upon the protein surface in the PFV experiment. These considerations still allow for a qualitative analysis, however. The E_m vs $f(I)$ data indicate that NE binds phosphate preferentially in the oxidized state, as the negative slope indicates that $|Z_{red}| < |Z_{ox}|$. NE should be slightly negatively charged at neutral pH due to its acidic isoelectric point near neutrality (pI = 6.7, as calculated from the amino acid sequence, and the a pI < 5.0 has been reported experimentally.)[54] Thus, reduction of the protein must also be coupled to a loss of overall negative charge. The plot of E_m vs $f(I)$ for HT displays a positive slope, suggesting that the binding of phosphate may not be specific to one oxidation

(50) Tezcan, F. A.; Winkler, J. R.; Gray, H. B. *J. Am. Chem. Soc.* **1998**, *120*, 13383−13388.
(51) Walker, F. A.; Huynh, B. H.; Scheidt, W. R.; Osvath, S. *J. Am. Chem. Soc.* **1986**, *108*, 5288−5297.
(52) Moore, E. C.; Reichard, P.; Thelander, L. *J. Biol. Chem.* **1964**, *239*, 3445−3452.
(53) Takayama, S. I. J.; Mikami, S. I.; Terui, N.; Mita, H.; Hasegawa, J.; Sambongi, Y.; Yamamoto, Y. *Biochemistry* **2005**, *44*, 5488−5494.
(54) Yamanaka, T.; Shinra, M. *J. Biochem.* **1974**, *13*, 1265−1273.

state. As an experimental pI of HT has not been determined, further experiments will be required to explore this issue. In our current study, the key observation for future studies is that the redox properties of NE and HT depend on phosphate ion concentration in a distinctive manner.

Conclusion

PFV studies have demonstrated the impact of the heme-binding loop 64 position upon the redox characteristics of cyts *c* from PA, HT, and NE. The potential for hydrogen-bonding interactions between the 64 position and Met61 can be rationalized by an upward shift in midpoint potential. Our experiments have underscored the fundamental differences in pH- and buffer-dependent behavior displayed by this collection of cytochromes and the impact the 64 position can have upon the influence of pH upon heme midpoint potential. We are now poised for further studies that will utilize PFV to explore the relationship between heme-binding loop sequence and redox thermodynamics observed in bacterial cyts *c*.

IC051003L